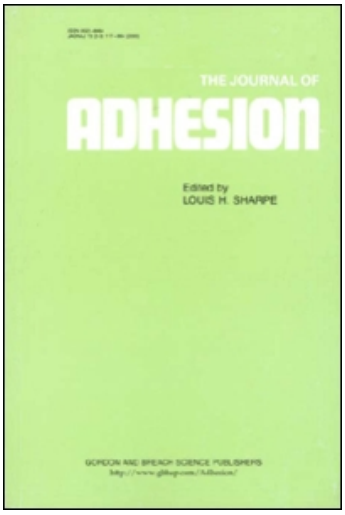

The Journal of Adhesion
Publication details, including instructions for authors and subscription information:
http://www.informaworld.com/smpp/title~content=t713453635

Electrochemical Sensors for Nondestructive Evaluation of Adhesive Bonds

G. D. Davis; L. A. Krebs[a]; L. T. Drzal[b]; M. J. Rich[b]; P. Askeland[b]
[a] DACCO SCI, INC., Columbia, MD, USA [b] Composites Materials and Structures Center, Michigan State University, East Lansing, MI, USA

To cite this Article Davis, G. D. , Krebs, L. A. , Drzal, L. T. , Rich, M. J. and Askeland, P.(2000) 'Electrochemical Sensors for Nondestructive Evaluation of Adhesive Bonds', The Journal of Adhesion, 72: 3, 335 — 358
To link to this Article: DOI: 10.1080/00218460008029289
URL: http://dx.doi.org/10.1080/00218460008029289

J. Adhesion, 2000, Vol. 72, pp. 335–358
Reprints available directly from the publisher
Photocopying permitted by license only

Electrochemical Sensors for Nondestructive Evaluation of Adhesive Bonds*

G. D. DAVIS[a, †], L. A. KREBS[a], L. T. DRZAL[b], M. J. RICH[b] and P. ASKELAND[b]

[a]*DACCO SCI, INC., 10260 Old Columbia Road, Columbia, MD 21046, USA;* [b]*Composites Materials and Structures Center, Michigan State University, East Lansing, MI 48824, USA*

(Received 6 July 1999; In final form 18 December 1999)

An *in-situ* corrosion sensor based on electrochemical impedance spectroscopy (EIS) has been used to detect moisture ingress into aluminum-aluminum and aluminum-composite adhesive bonds. Both wedge tests and tensile button tests (aluminum-aluminum bonds only) were performed. Upon moisture absorption, the impedance spectra change shape with the low-frequency region becoming resistive. The low-frequency impedance decreases by several orders of magnitude, depending on the adhesive and the experimental conditions. For bonds with stable interfaces, such as phosphoric acid anodized (PAA) aluminum, the absorbed moisture causes an initial weakening of the adhesive resulting in reduced strength or small crack propagation. A substantial incubation time prior to substrate hydration and bond degradation allows warning of potential joint deterioration and enables condition-based maintenance. For bonds with smooth interfaces with little or no physical bonding (mechanical interlocking), crack propagation can proceed interfacially with minimal moisture absorption. A comparison of the incubation times for Forest Products Laboratory (FPL, or sulfuric acid-sodium dichromate) etched surfaces, both bonded to epoxy adhesives and freely exposed to water or humidity at different temperatures, shows that hydration occurs with the same activation energy and, hence, the same mechanism, independent of whether or not the surface is covered with adhesive. However, the pre-exponential factor in the rate constant is dependent on the concentration of free moisture at the interface so that the hydration rate varies by several orders of magnitude.

---

*Presented at the 23rd Annual Meeting of The Adhesion Society, Inc., Myrtle Beach, South Carolina, USA, February 20–23, 2000. One of a Collection of papers honoring F. James Boerio, the recipient in February 1999 of *The Adhesion Society Award for Excellence in Adhesion Science, Sponsored by 3M.*

[†]Corresponding author. Tel.: 410-381-9475, Fax: 410-381-9643, e-mail: davis@daccosci.com

Keywords: Moisture; hydration; aluminum; electrochemical impedance spectroscopy; nondestructive evaluation; degradation

INTRODUCTION

Nondestructive inspection and evaluation (NDI, NDE) of adhesive bonds commonly requires separation of an interface or, in limited cases a "kissing" unbond that has intimate contact but no interfacial strength. It is currently not possible to nondestructively find weakened bonds or bonds in the process of degradation. Because the principal cause of environmentally-induced bond failure is moisture [1 – 5], one potential means to monitor such bond degradation is to track the ingress of moisture into the bondline. Depending on the properties of the bonded joint, moisture can promote these types of degradation mechanisms:

- Disruption of secondary interfacial bonds, *e.g.*, van der Waals forces.
- Weakening or disruption of primary interfacial bonds, *e.g.*, covalent or ionic bonds.
- Plasticization or weakening of the polymeric phase allowing disengagement of mechanical interlocking or physical interfacial bonds or failure within the polymer at stresses less than those required for a freshly-cured adhesive.
- Hydration or corrosion of a metallic adherend surface, destroying any chemical or physical interfacial bonds and forming corrosion products that add stresses to the bondline.

The details of each of these mechanism types will depend on the materials and surface treatments involved and the environmental conditions to which the system is exposed. For example, epoxy bonds to microscopically-smooth aluminum will fail according to the first mechanism very quickly upon exposure to moisture. In contrast, the failure of epoxy bonds to phosphoric acid anodized (PAA) aluminum [6 – 8] will fail according to the fourth mechanism, but only after an extended period. The severity of exposure conditions is generally increased by interfacial stresses, temperature extremes and cycles, ionic constituents, and humidity cycling.

Electrochemical impedance spectroscopy (EIS) has for many years been used to study absorption of moisture by coatings and the subsequent corrosion of the substrate under immersion conditions [9–15]. Traditionally, it has required remote counter and reference electrodes with access by the electrolyte to the polymeric surface. As such, it was not suitable for evaluation of adhesive bonds. In the most relevant adhesion study, Simpson and co-workers were able to correlate EIS measurements with paint adhesion by bonding pull stubs to painted surfaces after exposure to aggressive environments [16, 17]. Deflorian and Fedrizzi discussed how equivalent circuit elements derived from EIS data were related to moisture uptake and coating deadhesion [18]. Other researchers, as reviewed by Murray [19], have focused on correlating EIS measurements with different parameters, such as blister area or delamination from a scribe, which may be related to the adhesion of a paint coating, but are not relevant to a structural adhesive bond.

Davis *et al.*, used these conventional EIS measurements on an immersed half-joint specimen (aluminum adherend and epoxy adhesive without a second adherend) to study the adsorption of moisture by the adhesive and the eventual hydration of the aluminum surface [20, 21]. They conclusively showed that hydration of a Forest Products Laboratory (FPL, or sulfuric acid-sodium dichromate etched) aluminum adherend [8, 22] would occur under an adhesive film and that the hydration products would be capable of inducing bond failure due to their increase in volume.

The application of EIS to coated specimens in ambient conditions has been advanced recently with the development of an *in-situ* corrosion sensor that acts as both the counter and reference electrodes and allows EIS spectra to be obtained in air [23–28]. It has been used to detect moisture absorption and substrate corrosion for coated metals and composite materials (moisture absorption only). Here, we report on the application of this technology to adhesive bonds using both wedge tests (ASTM D3762) and tensile button tests (ASTM D4541) using a pneumatic adhesion tensile testing instrument (PATTI). Moisture ingress was tracked with EIS with bonds exposed mostly to high humidity although immersion was used in a few cases. Because the stability of an aluminum bond once moisture is present is governed by the surface treatment of the adherend surface [3, 4, 29],

different treatments were evaluated. These treatments ranged from smooth with poor expected performance (polished or sanded) to microscopically rough with excellent expected performance (PAA).

EXPERIMENTAL

Specimen Preparation

Surface preparation of the 2024-T6 aluminum adherends included PAA [6–8], the FPL etch [8, 22], sand or grit blasting, and sanding/polishing. The polished aluminum substrates were prepared using a wet polishing method on a rotating metallographic polisher. Samples were polished for 3 minutes each using 1000, 2400 and 4000 polishing papers and immediately dried with a soft paper tissue after the final step. This polishing sequence produced a flat, optically-reflective surface.

The four surface preparations span a wide range of surface morphology and stability and, thus, depend to different degrees on mechanical interlocking (physical bonding) and secondary bonds (*e.g.*, van der Waals forces) to bond to the epoxy adhesives. The PAA surface, which is the current "best practice" treatment for bonding to aluminum, is stable against hydration [30] and has a highly evolved, open porous oxide structure of the order of tens of nanometers [31]. It provides the greatest density of high-quality physical bonds at the interface. The FPL surface, which was widely used in the past for aerospace bonding and still is occasionally used, is less stable against hydration [32] and has a shallow porosity of the order of tens of nanometers [31]. A grit-blasted surface, which can be used for less demanding bonding applications, has a simpler, larger scale morphology of the order of tens of micrometers. Its physical bonds are of lower quality and density. The polished surface is smooth and exhibits very little, if any, physical bonding.

Some Al–Al wedge test specimens were prepared as $6.5'' \times 6'' \times 0.125''$ (165 mm × 150 mm × 3.2 mm) panels which were subsequently cut into six $1'' \times 6''$ (25 mm × 150 mm) strips. Others were prepared as individual $1'' \times 6''$ (25 mm × 150 mm) strips. A limited number of Al-graphite/epoxy and Al-glass/epoxy specimens were also

individually prepared. Composite panels were autoclave processed prior to bonding to the aluminum substrate. Woven fiberglass prepreg was SP Systems E293 epoxy with 7781 glass fiber, and the carbon fiber woven prepreg was Hexcel AS4 fiber in 8552 epoxy. Both of these prepreg formulations are used as structural laminates in aerospace parts. A standard 350°F-85 psi (177°C – 0.59 MPa) process schedule was used to consolidate the panels prior to the manufacture of the wedge coupons. The smooth composite surface processed against the cull plate was selected for bonding to the aluminum substrate. Both Cytec FM-73 and FM-300 adhesives were used. The FM-73 is a 250°F (121°C)-curing adhesive that exhibits moderate moisture uptake. The FM-300 is a 350°F (177°C)-curing adhesive that absorbs less moisture. Two adhesive plies were used. For the aluminum/adhesive/composite samples, 6″ × 6″ (150 mm × 150 mm) lay-ups were processed in a static press preheated to the temperature appropriate for each film adhesive and processed at a pressure of 40 PSI (0.28 MPa) for one hour. To prevent a metal wedge from electrically shorting the two adherends, Delrin® acetal resin or polycarbonate wedges were used. After the wedges were driven and the initial cracks allowed to equilibrate, the specimens were placed in humidity chambers operating at 60°C and 95–98% RH. Periodically, they were removed from the chamber and shaken or blown dry with compressed air to remove excess condensed moisture. The crack length was marked and EIS measurements taken (see below).

Tensile button tests were performed on 2″ × 2″ × 0.125″ (50 mm × 50 mm × 3.2 mm) panels prepared as described above. The Al stubs were PAA-treated to force any moisture degradation to the panel interface. The adhesive was 3M DP460 two-part epoxy. Glass beads (45–90 μm in diameter) were used to provide a uniform bond thickness and prevent electrical contact between the stub and the panel. To assure uniform, complete cure, prior to any humidity exposure, the specimens were baked at 90°C for 30 minutes prior to testing. Initial bond strengths were determined using the PATTI tester on 2–3 specimens for each surface treatment. The remaining specimens were placed in high humidity (50°C, 95% RH). Periodically, specimens were removed and inspected using the *in-situ* corrosion sensor technology (see below). The bond strengths were measured on selected specimens following different periods of exposure. After

approximately three months, the specimens were removed from the humidity and placed in warm (50°C) water in an attempt to accelerate the degradation process while the inspection and testing procedures continued.

EIS Measurements

Temporary *in-situ* corrosion sensor electrodes were applied to each adherend of the wedge tests using conductive pressure-sensitive tape and to the stub and substrate of the PATTI tests using mechanical fasteners when the specimens were removed from the humidity or immersion conditions and monitored. For convenience in these experiments, the sensors were removed following the measurements prior to reinsertion into the exposure environment. The sensor electrodes serve as the counter and working electrodes for the EIS measurements. A separate reference electrode is not used. The sensors allow conventional EIS data acquisition in ambient environments instead of the immersion conditions required by traditional remote electrodes.

EIS measurements were taken using either a Gamry PC3 Portable Potentiostat/Galvanostat with CMS100/105/300 Corrosion Measurement System (tensile buttons) or a CH Instruments model 650A electrochemical workstation (wedge tests). The Gamry is optimized for rapid data acquisition (*e.g.*, Fig. 1) while the CH Instruments is optimized for high signal-to-noise ratio (*e.g.*, Fig. 8). The impedance spectra were acquired over the range of approximately 0.1 Hz to 5,000 Hz. The spectra were customarily evaluated in the Bode magnitude plots (impedance magnitude *vs.* frequency). Bode phase angle plots (phase angle *vs.* frequency) were used to confirm interpretation of the magnitude plots. The low frequency region of the impedance spectrum is very sensitive to moisture ingress, as discussed below. The geometric mean of the lowest-frequency decade (three to six points) was used to improve the signal-to-noise ratio compared with use of a single frequency. This averaging was particularly important for the Gamry data, which inherently had a lower signal-to-noise ratio.

Impedance spectra were obtained on several tensile button specimens (up to the point that a given button was pulled) and at least two wedge test specimens. The impedance trends for tensile button

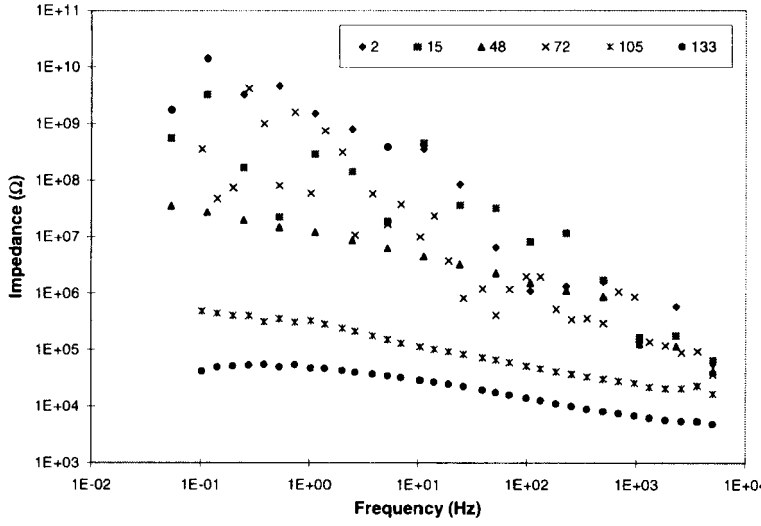

FIGURE 1 Impedance spectra for a PAA tensile specimen with one of the largest uptakes of moisture. The number of days is given in the legend.

specimens were very similar as reflected in Figures 4 and 6, which are compilations of eight to nine specimens for each treatment. The impedance trends for wedge test specimens were also similar for a given surface treatment. The data shown in Figures 11 and 12 represent two wedge test specimens.

RESULTS

Tensile Button Tests

A typical series of impedance spectra for the tensile button tests is given in Figure 1. Initially, the spectra are capacitive in nature (slope of -1 on the log impedance *vs.* log frequency graph) with high impedance at low frequencies. This behavior is similar to that of a good protective coating and reflects a polymer with no pathways of low resistance. As the adhesive absorbs moisture, the low-frequency spectrum decreases in impedance and becomes resistive or independent of frequency. This behavior reflects moisture ingress into the pores of a polymer and formation of pathways of relatively low resistance. It is typical of a protective coating in the process of degradation.

The decrease of the low-frequency impedance for this specimen is shown in Figure 2 and reflects the absorption of moisture. This specimen exhibited a fairly steady impedance decrease (aside from one measurement which was of poorer quality than the rest). Other specimens exhibited smaller decreases or a plateau, but the same general trend, depending on microdifferences in the humidity chamber or small differences in the specimens. For these measurements, the data are dominated by the region of the specimen with the lowest impedance. In this case, the data represent the impedance of the near-edge region of the bondline where moisture saturation first occurs.

The EIS spectra can be modeled with an *RC* circuit, such as the typical coated metal circuit of Figure 3, where R_{po} and C_c represent coating properties, R_{cor} and C_{DL} represent interfacial properties, and R_{sol} represents the solution resistance (not relevant in this case). The dry specimen would have a very high R_{po} value so that C_c dominates the spectrum. As moisture is absorbed, the R_{po} value would decrease by several orders of magnitude and begin to dominate at low frequencies when the impedance associated with C_c is very high. The C_c value would also increase (the impedance associated with the capacitor would decrease), but on a much smaller scale, because of the larger dielectric constant of water compared with the adhesive.

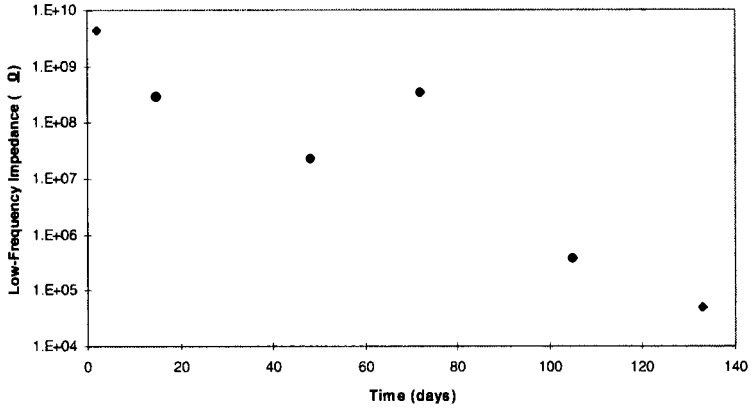

FIGURE 2 Geometric mean of the low frequency impedance as a function of exposure time for the PAA-treated button pull specimen of Figure 1. The lowest three-to-five frequency points (corresponding to the lowest decade of frequencies) was used in the geometric mean.

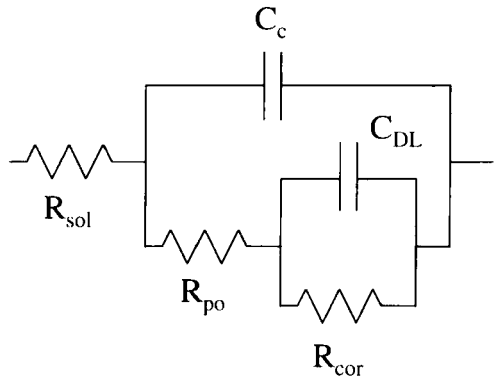

FIGURE 3 Typical equivalent circuit for a coated metal. The pore resistance and coating capacitance, R_{po} and C_c, respectively, correspond to coating properties. The corrosion resistance and double-layer capacitance, R_{cor} and C_{DL}, respectively, correspond to interfacial properties. The solution resistance, R_{sol}, is shown for completeness, but is not a factor with the corrosion sensor.

Initially, the interfacial parameters would remain unchanged. These parameters would reflect adherend hydration or other interfacial reactions once they occur.

The effect of this moisture absorption on the tensile pull strength strongly depends on the surface treatment. This dependence is illustrated in Figure 4. The initial decrease in pull strengths from approximately 38 MPa to 27 MPa corresponds to a decrease in the cohesive strength of the adhesive as moisture is absorbed. This decrease is independent of surface treatment. For PAA specimens, the length of time available for this experiment (approximately five months) under these conditions (humidity, followed by immersion) was insufficient to induce hydration. Accordingly, the microcomposite interphase formed by the porous PAA oxide [31] and the adhesive remained stable and stronger than the cohesive strength of the adhesive so that failure was almost entirely within the adhesive (Fig. 5). Similar behavior was also observed for grit-blasted and FPL-etched specimens (Fig. 6), with the exception of an FPL surface at the end of the experiment where the strength decreased by approximately 50% and partial interfacial failure occurred. XPS analysis of the interfacial region of this specimen showed that, where failure was interfacial, hydration had occurred under the adhesive. In contrast, because the sanded surfaces exhibit no evolved

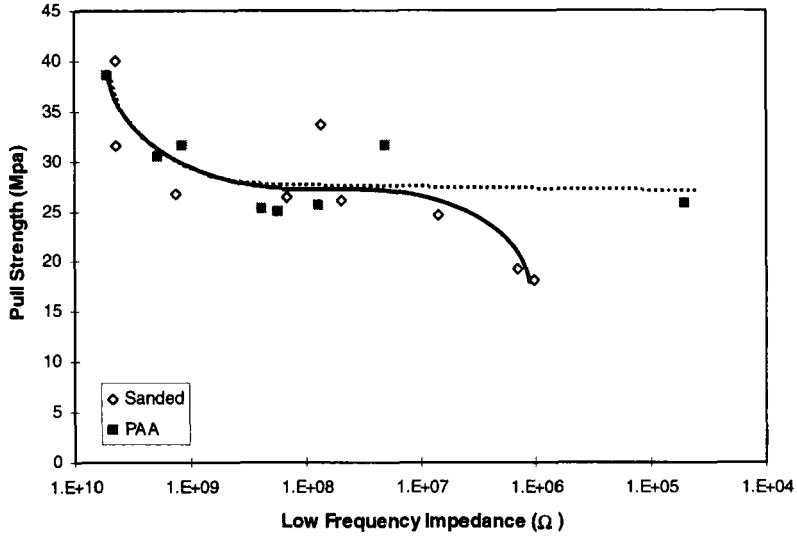

FIGURE 4 Tensile pull strengths as a function of the geometric mean of the low-frequency impedance for PAA and sanded aluminum surfaces. The low-frequency impedance was obtained shortly before the button was pulled in all cases. The data represent nine different specimens.

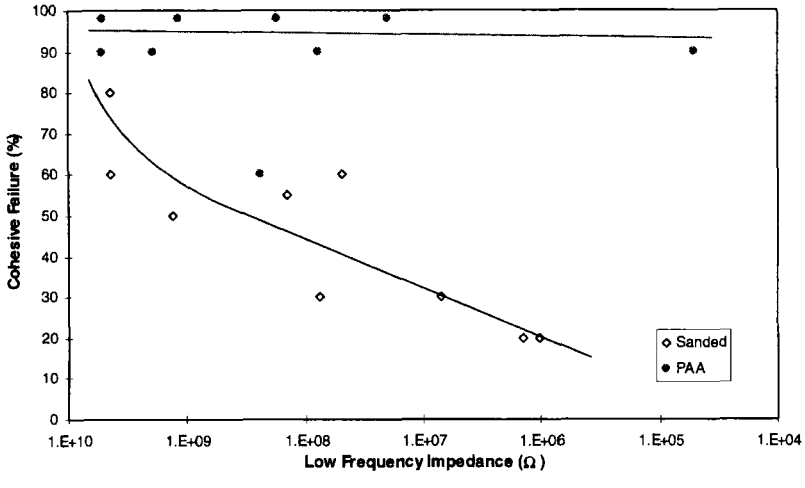

FIGURE 5 Percentage of cohesive failure (visual) in the adhesive as a function of the geometric mean of the low-frequency impedance for PAA and sanded aluminum surfaces. The low-frequency impedance was obtained shortly before the button was pulled in all cases. The data represent nine different specimens.

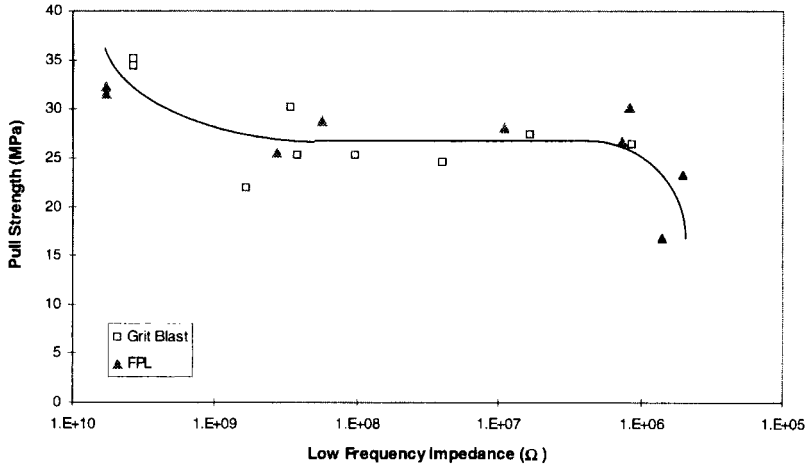

FIGURE 6 Tensile pull strength as a function of the geometric mean of the low-frequency impedance for grit blasted and FPL-etched aluminum surfaces. The low-frequency impedance was obtained shortly before the button was pulled in all cases. The data represent nine different specimens.

microroughness, their bonds to the epoxy adhesive rely more on secondary bonds, such as van der Waals forces, which are readily disrupted by moisture. The locus of failure gradually shifts to increasingly more interfacial with the interfacial region beginning along one segment of the edge and growing along the circumference and toward the center. Although the interface is weakened considerably by the moisture, it still retains some strength as indicated by Figure 7 where the extrapolated pull strength at 0% cohesive failure (100% interfacial failure) is approximately 15 MPa. By comparison, the dry interfacial strength must be at least 40 MPa or else the interface would be the weakest link of the bond.

Wedge Tests

Joints tested in the wedge test configuration exhibit similar behavior to the PATTI specimens as indicated in Figure 8. Initially, the adhesive shows completely capacitive behavior. As moisture is absorbed, the low-frequency region of the spectra becomes resistive in nature with the extent of the resistive region generally increasing in frequency extent as more moisture is absorbed. The geometric mean of the

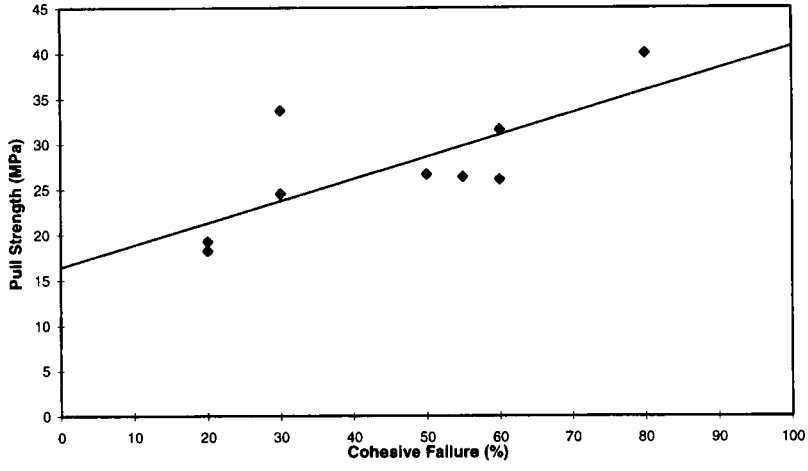

FIGURE 7 Tensile pull strength as a function of percentage of cohesive failure (visual) for sanded aluminum surfaces. Each point represents a different specimen.

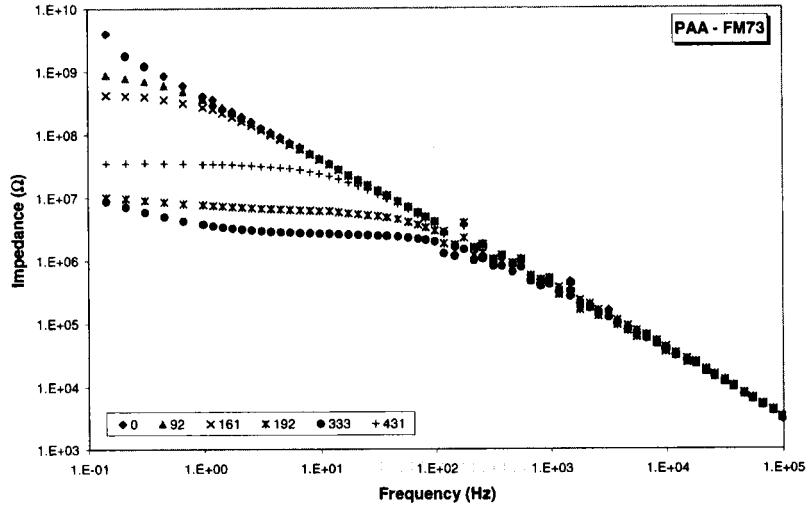

FIGURE 8 EIS spectra of a PAA wedge test using FM-73 adhesive. The humidity exposure ranged from 0 to 430 hours and is given in the legend.

low-frequency impedance is given in Figure 9. Although there is considerable scatter, the data show a two-decade decrease in the low-frequency impedance between 100 and 200 hours as the adhesive

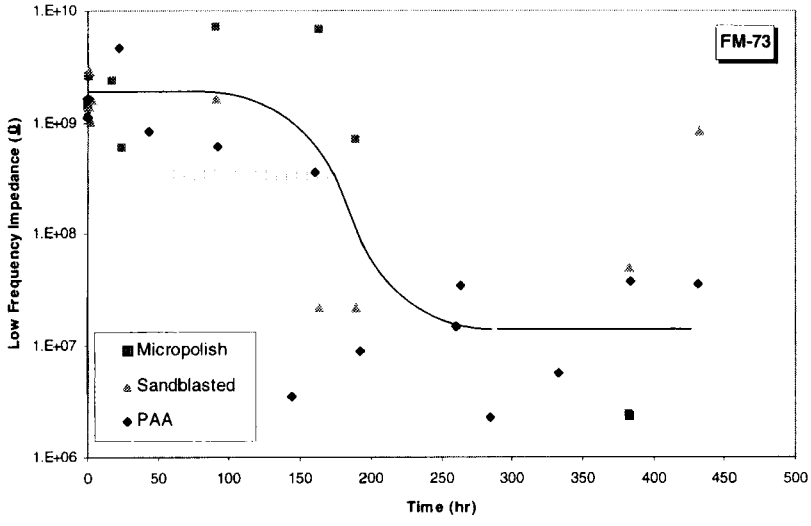

FIGURE 9 Geometric mean of the impedance over the lowest frequency decade for micropolished, sandblasted, and PAA aluminum wedge specimens using FM-73.

absorbs moisture. Because the moisture uptake is governed by the adhesive, there is little dependence on surface preparation. The PAA specimens consistently exhibit slightly lower impedance than the other two treatments. This may be reflective of the lower crack length of the PAA specimens. At small crack lengths, the adhesive at the crack tip is subject to tensile stresses that increase the free volume of the polymer and allow more moisture absorption. An even greater dependence of the impedance (moisture absorption) on crack length was previously observed for FPL adherends bonded with FM123 adhesive [21].

Crack length measurements are given in Figure 10. Two distinct behaviors are noted, depending on surface preparation. All start cohesively between the two FM-73 plies. The crack in the PAA specimens remains between the two adhesive films and only slowly propagates. Its interface remains stable under these conditions, as expected. The cracks for the other two treatments very quickly shift to the interface. The smooth interface of the micropolished adherends can withstand very little stress and the crack propagates almost to the end of the specimen upon exposure to humidity as the moisture disrupts the secondary interfacial forces. The sandblasted specimens are able to support some interfacial stress as a result of low-quality

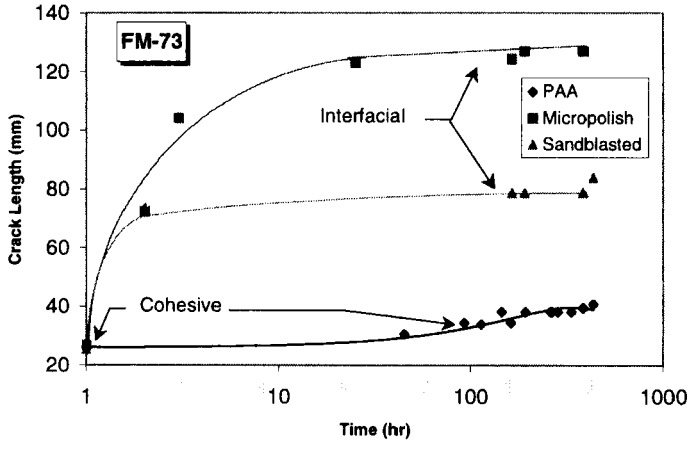

FIGURE 10 Crack length *vs.* time for FM-73 wedge test specimens. The data represent two individual specimens.

roughness and the crack rapidly advances to the point where the limiting stress is reached.

Comparing the EIS measurements with crack lengths shows two different types of correlations, depending on the locus of crack propagation (Fig. 11). For sandblasted and micropolished specimens, for which the crack propagates interfacially, the initial, rapid crack growth occurs with minimal change in the low-frequency impedance. For these weak interfaces, the crack propagates as soon as moisture reaches the interface – before it has a chance to absorb into the bulk adhesive and change the impedance. Over time, this absorption occurs and the impedance decreases, but the crack has arrested or is growing very slowly as it reaches the point of sustainable stress. For the PAA specimens, the limiting factor governing crack propagation under these conditions and time is not the interface but, rather, it is the weakening of the adhesive due to moisture absorption. In this case, there is a distinct relationship between the low-frequency impedance (absorbed moisture) and crack growth until the crack arrests after approximately one centimeter of propagation. At that point, the adhesive continues to absorb moisture, but without additional crack growth.

Similar results were obtained with wedge tests using FM-300 adhesive except that these specimens exhibit less moisture absorption by the adhesive and, hence, a smaller decrease in the low-frequency

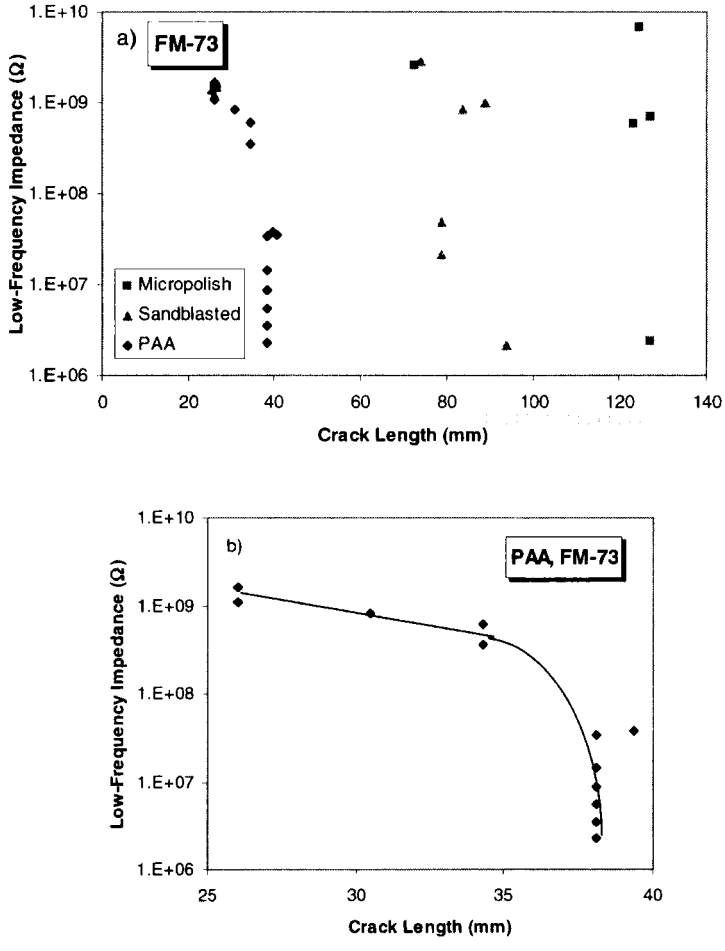

FIGURE 11 Geometric mean of the low frequency impedance as a function of crack length for FM-73 adhesive. (a) all three surface treatments; (b) increased scale for PAA only. Data for two specimens are shown for each surface treatment.

impedance of the EIS spectra. Again, the interfacial crack propagation of the sand-blasted and micropolished specimens allowed crack growth before there was significant absorption of moisture by the adhesive. On the other hand, moisture absorption appeared to be a prime factor in crack propagation within the adhesive for the PAA specimens as reflected by the correlation in Figure 12.

A limited number of experiments were performed using PAA aluminum adherends bonded to either glass fiber-reinforced (epoxy)

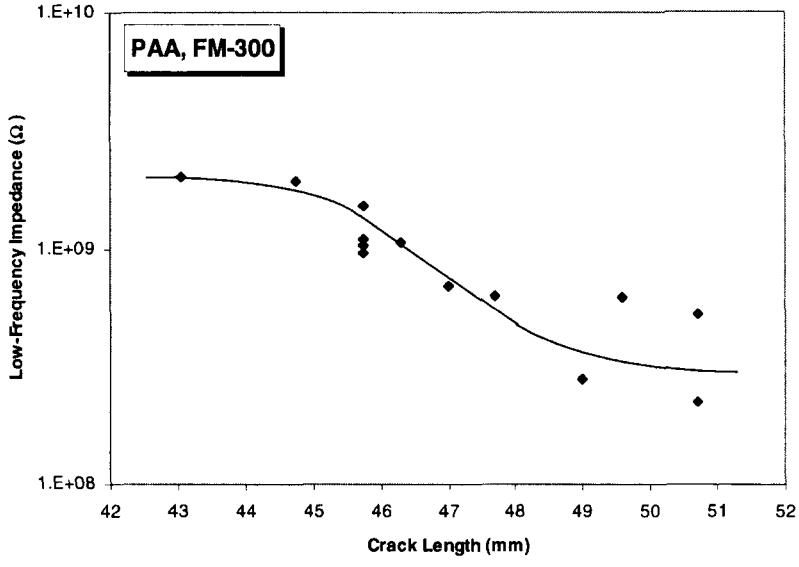

FIGURE 12 Geometric mean of the low frequency impedance as a function of crack length for PAA specimens with FM-300 adhesive.

composites (GFC) or carbon fiber-reinforced (epoxy) composites (CFC). Crack propagation for these specimens was within the composite near the adhesive interface. The interface with the adhesive was not the limiting factor for these specimens under these conditions.

The EIS measurements reflect both the adhesive and the composite. The greater impedance of the GFC data (Fig. 13) compared with that of the CFC data (Fig. 13) and that of the aluminum/aluminum data (Fig. 9) indicate that the impedance of the glass composite is dominating over that of the adhesive. By comparison, the lower impedance (greater conductivity) of the graphite epoxy is evident. There is a small, but distinct, trend for the impedance of the GFC specimens to decrease over time. We attribute this to absorption of moisture by the composite itself. Detection of moisture absorption in both GFC and CFC monolithic material has been previously reported using the *in-situ* sensors [33]. Based on the previous data, the amount of moisture absorbed by the GFC under these conditions is small, less than 1%. No indications of moisture absorption in the CFC are seen, but moisture detection in these materials has required equivalent circuit analysis which was not done in this case.

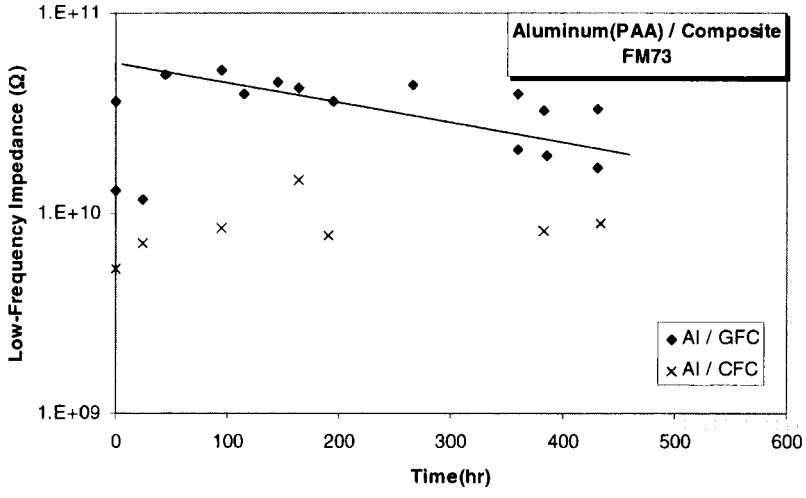

FIGURE 13 Geometric mean of the low-frequency impedance as a function of time for aluminum/glass fiber-reinforced composites and aluminum/carbon fiber-reinforced composites.

DISCUSSION

The utility of tracking moisture adsorption in a bondline as a means of health monitoring an adhesive joint is dependent on the surface preparation of the adherends and the resulting failure mechanism. The use of EIS or other moisture-sensitive probes is best suited for situations where relatively long exposure to moisture results in joint failure from plasticization or other weakening of the adhesive or from hydration or other corrosion of the adherend surface. PAA adherends are one example in which these conditions are met. For these joints, the impedance spectrum significantly changes in shape and the low-frequency impedance decreases by one to three orders of magnitude (depending on the adhesive) well before hydration of the oxide and joint failure. Thus, there is ample time to warn of impeding bond degradation and preventative action can be taken.

This ability to warn is in contrast to the situation with polished or sandblasted adherends where crack propagation occurs interfacially with the very first ingress of moisture to the interface. The smooth adherends, without a high density of physical bonds, fail as soon as a

small amount of moisture reaches the interface. There is no need for the adhesive to absorb moisture and for the moisture to be in contact with the interface for an extended period of time. Fortunately, these types of surface preparations and the resulting bonds are not used where strong, durable joints are required. Structures for which these bonds are acceptable would not be candidates for bondline health monitoring.

It is interesting to compare the time scales required for degradation in these experiments and similar experiments. The tensile button tests lasted up to 183 days or approximately 6 months in high humidity and subsequent water immersion. During that time, the sanded specimens showed definite degradation; the PAA specimens showed minimal adhesion strength decrease and no signs of interfacial degradation; and one FPL specimen showed partial interfacial failure towards the end. For these specimens, moisture has to diffuse into the adhesive from the edges without scrim cloth or other medium that might aid moisture ingress. The first effect of the moisture is to weaken the adhesive and this was observed for all surface treatments (Figs. 4 and 6).

Subsequent degradation occurs as the moisture reaches the interface and begins to react with the interfacial bonds and the aluminum oxide. The rate at which interfacial degradation occurs depends on the quality and quantity of physical bonds (mechanical interlocking) between the oxide and polymer and the stability of the oxide against hydration. For interfaces with minimal physical bonds, such as the sanded specimens, bond failure occurs relatively rapidly, but still requires sufficient moisture to reach the interface. In the other extreme, PAA interfaces have very evolved physical bonds which are disrupted only after the oxide slowly hydrates [29–31]. This combination serves to provide excellent durability under service conditions and requires even accelerated tests like this one to take a long time for degradation to occur. Intermediate between these two extremes is the FPL surface. It has less evolved physical bonds and only fair resistance to hydration [29, 31, 32].

A comparison can be made for the times for hydration to occur, t_i, for FPL surfaces under different conditions. In this experiment where moisture had to diffuse from the edge of an adhesive, one specimen showed hydration beginning after 140 days; others showed no hydration after 120 and 135 days. The 140-day period represents a

minimum value of the incubation time at 50°C under these conditions. For specimens covered with an epoxy adhesive, but with a free epoxy surface exposed to water at 58°C so that moisture only had to absorb through the thickness of the adhesive, Davis *et al.*, found hydration beginning after approximately 110 days [20]. At 75°C, the incubation time decreased to approximately 229 hours [34]. For bare specimens, the incubation time is much shorter. McNamara and Agoff found incubation times to range from 3 minutes at 70°C to 85 minutes at 40°C for immersion; for humidity, the times ranged from 5 hours at 45°C to 27 hours at 35°C [35]. These data are compiled on the Arrhenius plot of Figure 14 for the equation

$$\frac{1}{t_i} \propto k = Ae^{-E_a/RT}.$$

Based on the immersed, bare substrates, the activation energy, E_a, which is proportional to the slope, is calculated to be 82 kJ/mole. This value compares well with that determined by Alwitt of 78 kJ/mole for hydration of the amorphous oxide on pure Al [36]. Within the

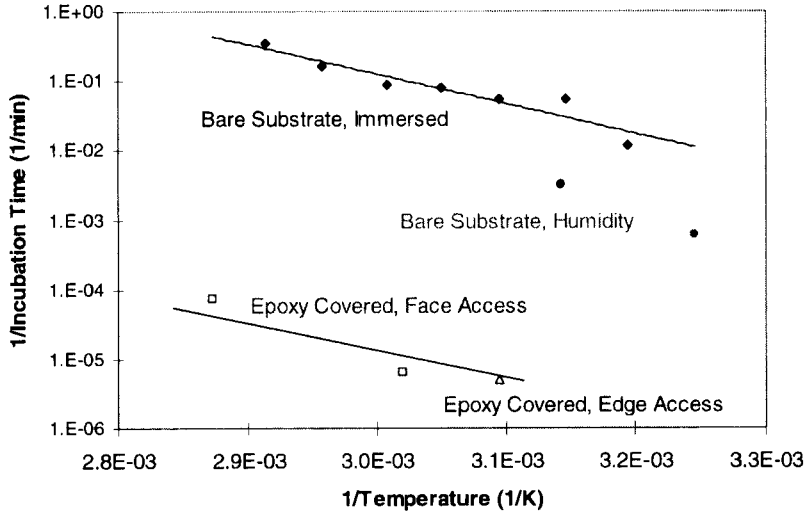

FIGURE 14 Arrhenius plot of incubation times prior to hydration of FPL aluminum under various conditions. The bare-substrate data are from Ref. [35]; the epoxy-covered, face-access data are from Refs. [20] and [34]; the epoxy-covered, edge-access datum is from the current work.

accuracy of the limited data, the activation energy for hydration is the same for each condition. This indicates that the same mechanisms control hydration of bare FPL surfaces and FPL surfaces within an adhesive bond and that the adhesive serves only to slow the hydration process by reducing the amount of water present at the surface (see below). Although not available from the data reported here, the activation energy for hydration of a PAA surface would be much higher so that the incubation time would be much longer for identical conditions. Previous experiments indicate that the incubation time for PAA surfaces is approximately two orders of magnitude longer than that for FPL surfaces [37]. Accordingly, it is not surprising that we did not detect any hydration of the PAA tensile-button specimens during our testing.

The pre-exponential factor, A, is a function, among other factors, of the concentration of water available for reacting with the surface. As a result, the rate constant, k, varies dramatically with experimental conditions. The most water is available in immersion and the rate constant is correspondingly highest (incubation time is shortest). Even though a thin film of condensed moisture may have been present on the humidity-exposed specimens all or part of the time, the amount of water available for reaction is less and this reduction is reflected in the smaller rate constant (longer incubation time). The lowest amount of water available is when the surface is covered with epoxy. A typical epoxy can absorb 1–2.5% moisture, but not all of this moisture is available to react with the surface – much of it will be bound to the polymer *via* hydrogen bonding. Consequently, the reduction of approximately three orders of magnitude in incubation times for bare surfaces exposed to humidity and epoxy-covered surfaces is reasonable.

The small rate constant for hydration of epoxy-coated specimens and the slow rate of bond degradation for the tensile button specimens demonstrate the limitations of using short-term lap shear, tensile button, or similar joint configurations to test the durability of surface preparations. Failure of poorly-prepared surfaces, as denoted by interfacial failure of the sanded specimens, was detected in our experiments after one to two months. Failure of FPL-etched surfaces, which exhibit the poorest durability of any commonly-used, high-performance surface treatment of structural aluminum joints, began to

occur only toward the end of the five-month exposure. No failure was observed for the PAA specimens that should show the best durability. Based on differences in the incubation times, we would expect the PAA specimens to begin to fail only after approximately five years. The addition of primers and other common procedures would further delay hydration and bond failure and is reflected in the long-term success of the PAA treatment for aircraft and other structures.

Discrimination of surface treatments based on wedge tests is much more rapid, as is widely practiced. For example, FPL adherends typically show interfacial failure after a few hours in wedge tests as opposed to 140 days for the tensile buttons. A one-week wedge test allows ready distinction between different surface treatments, and often the differences are apparent after only 24 hours. The tensile button tests were just beginning to show a distinction after five months.

SUMMARY AND CONCLUSIONS

Electrochemical impedance spectroscopy (EIS) measurements using an *in-situ* corrosion sensor were able to detect the absorption of moisture in adhesive joints in the wedge test and tensile button configurations. For high-performance surface treatments, such as phosphoric acid anodization (PAA), where there is a high density of physical bonds and the oxide is resistant to hydration, the low-frequency impedance values correlate with bond performance and give substantial warning before hydration and joint failure ultimately occurs. This warning would enable condition-based maintenance where remedial action or repair can be scheduled before irreversible, environmentally-induced bond degradation becomes serious. For smooth surfaces with little or no opportunity for mechanical interlocking, bond failure can begin as soon as moisture reaches the interface, especially in cases of opening stresses, such as a wedge test. In these cases, little warning is available from the EIS measurements. However, these treatments are not used in critical bondlines where durability in moist conditions is required. Such structures would not be candidates for health monitoring.

In the case of composite/aluminum bonds, the EIS measurements are reflective of both the adhesive and the composite. For glass fiber-reinforced composites (GFC), the composite dominates the signal

and moisture ingress into the GFC can be detected. For carbon fiber-reinforced composites, the conductive nature of the graphite fibers complicates the signal and more sophisticated data analysis is needed.

An analysis of the failure modes and incubation times for hydration of FPL surfaces within a bond and freely exposed to moisture under a variety of conditions reconfirms that hydration of the aluminum surface occurs in a joint and is the primary cause of moisture-induced interfacial failure. The data show that the activation energy for hydration of an FPL surface is the same whether or not the surface is covered with adhesive. This indicates that the same hydration mechanisms are occurring. In contrast, the rate constant, which also depends on the concentration of water at the interface, among other factors, is very different for bare surfaces and surfaces within a joint. The reaction rate will be three to four orders of magnitude slower within a joint that has no opening stresses. These kinetics must be taken into account in the design of experiments to test surface preparations.

Acknowledgements

This work was funded by AFOSR under contract FQ8671-98-1402. We are grateful for Dave McNamara sharing some of his unpublished results and for Cytec providing some of the adhesives. We are also appreciative of the technical assistance of Craig Bevans, Tom Longazel and Duane Stuart.

References

[1] Comyn, J., "Kinetics and Mechanism of Environmental Attack", In: *Durability of Structural Adhesives*, Kinloch, A. J. Ed. (Applied Science, London, 1983), p. 85.
[2] Davis, G. D., "Surface Considerations", In: *Handbook on Engineered Materials Vol. 3: Adhesives and Sealants*, Brinson, H. F., Ch. (ASM International, Metals Park, OH, 1990), p. 235.
[3] Kinloch, A. J., *Adhesion and Adhesives: Science and Technology* (Chapman and Hall, London, 1987).
[4] Minford, J. D., *Handbook of Aluminum Bonding Technology and Data* (Marcel Dekker, New York, 1993).
[5] Davis, G. D. and Shaffer, D. K., In: "Durability of Adhesive Joints", *Handbook of Adhesive Technology*, Mittal, K. L. and Pizzi, A. Eds. (Marcel Dekker, New York, 1994), p. 113.

[6] Kabayashi, G. S. and Donnelly, D. J., Report D6-41517, The Boeing Company, 1974.
[7] Marceau, J. A., "Phosphoric Acid Anodize", In: *Adhesive Bonding of Aluminum Alloys*, Thrall, E. W. and Shannon, R. W. Eds. (Marcel Dekker, New York, 1985).
[8] Wegman, R. F., *Surface Preparation Techniques for Adhesive Bonding* (Noyes, Park Ridge, NJ, 1989).
[9] Mansfeld, F., *Corrosion* **37**, 301 (1981).
[10] Kendig, M., Mansfeld, F. and Tsai, S., *Corros. Sci.* **23**, 317 (1983).
[11] Kendig, M. and Scully, J., "Basic Aspects of the Application of Electrochemical Impedance for the Life Prediction of Organic Coatings on Metals", *Corrosion89* Paper 32, NACE (1989).
[12] Scully, J. R., *J. Electrochem. Soc.* **136**, 979 (1989).
[13] Tait, W. S., *J. Coat. Technol.* **61**, 57 (1989).
[14] Murray, J. N. and Hack, H. P., "Long Term Testing of Epoxy Coated Steel in ASTM Sea Water Using EIS", *Corrosion90* Paper 140, NACE 1990.
[15] Grandle, J. A. and Taylor, S. R., *Corrosion* **50**, 792 (1994).
[16] Simpson, T. C., Hampel, H., Davis, G. D., Arah, C. O., Fritz, T. L., Moran, P. J., Shaw, B. A. and Zankel, K. L., *Prog. Organic Coatings* **20**, 199 (1992).
[17] Davis, G. D., Shaw, B. A., Arah, C. O., Fritz, T. L., Moshier, W. C., Simpson, T. C., Moran, P. J. and Zankel, K. L., *Surf. Interface Anal.* **15**, 107 (1990).
[18] Deflorian, F. and Fedrizzi, L., *J. Adhes. Sci. Technol.* **13**, 629 (1999).
[19] Murray, J. N., "EIS and Organic Coating Adhesion/Disbondment: A Review with Supplementary Data", *Proc. CORROSION/97 Research Topical Symposia* (NACE, Houston, TX, 1997), p. 177.
[20] Davis, G. D., Whisnant, P. L. and Venables, J. D., *J. Adhes. Sci. Technol.* **9**, 433 (1995).
[21] Davis, G. D., Whisnant, P. L. and Wolff, J. P. Jr., *Proc. 41st Inter. SAMPE Symp.* (SAMPE, Covina, CA 1996), p. 544.
[22] Eichner, H. W. and Schowalter, W. E., Report 1813, Forest Products Laboratory, 1950.
[23] Davis, G. D. and Dacres, C. M., "Electrochemical Sensors for Evaluating Corrosion and Adhesion on Painted Metal Structures", U.S. Patent 5,859,537 (January, 1999).
[24] Davis, G. D. and Dacres, C. M., "Portable, Hand-Held *in-situ* Electrochemical Sensor for Evaluating Corrosion and Adhesion on Coating or Uncoated Metal Structures", patent pending.
[25] Davis, G. D., Dacres, C. M., Shook, M. and Wenner, B. S., In: *Proc. Workshop on Intelligent NDE Sciences for Aging and Futuristic Aircraft*, Ferregut, C., Osegueda, R. and Nuñez, A. Eds. (El Paso, TX, 1997), p.141.
[26] Davis, G. D., Dacres, C. M. and Shook, M. B., In: *Nondestructive Evaluation of Utilities and Pipelines II*, Reuter, W. G. Ed., Proc. SPIE Vol. 3398 (Society for Photo-optical Instrumentation Engineers, Bellingham, WA, 1998), p. 92.
[27] Davis, G. D., Dacres, C. M. and Krebs, L. A., "*In-situ* Corrosion Sensor for Coating Testing and Screening", *Materials Performance* **39**(2), 46 (2000).
[28] Davis, G. D., Dacres, C. M. and Krebs, L. A., "EIS-Based *in-situ* Sensor for the Early Detection of Coating Degradation and Substrate Corrosion", *Corrosion2000*, Paper 275 (NACE, Houston, TX, 2000).
[29] Clearfield, H. M., McNamara, D. K. and Davis, G. D., "Surface Preparation of Metals", *Handbook on Engineered Materials, Vol. 3: Adhesives and Sealants*, Brinson, H. F., Ch. (ASM International, Metals Park, OH, 1990), p. 259.
[30] Davis, G. D., Sun, T. S., Ahearn, J. S. and Venables, J. D., *J. Mater. Sci.* **17**, 1807 (1982).
[31] Venables, J. D., McNamara, D. K., Chen, J. M., Sun, T. S. and Hopping, R. L., *Appl. Surf. Sci.* **3**, 88 (1979).

[32] Ahearn, J. S., Davis, G. D., Sun, T. S. and Venables, J. D., In: *Adhesion Aspects of Polymer Coatings*, Mittal, K. L. Ed. (Plenum Press, New York, 1983), p. 281.
[33] Davis, G. D., Dacres, C. M., Krebs, L. A. and Bevans, C. E., *Proc. 4th DOD Composites Repair Technology Workshop, Vol. 1.* (Santa Fe, NM, 1998).
[34] Davis, G. D. and Whisnant, P. L., unpublished work, Lockheed Martin Laboratories, 1995.
[35] McNamara, D. K. and Agoff, E., unpublished work, Martin Marietta Laboratories, 1981.
[36] Alwitt, R. S., *J. Electrochem. Soc.* **121**, 1322 (1974).
[37] Davis, G. D. and Venables, J. D., "Surface and Interfacial Analysis", In: *Durability of Structural Adhesives*, Kinloch, A. J. Ed. (Applied Science, Essex, 1983), p. 43.